Intermittency and coherent structures in two-dimensional turbulence

1986 J. Phys. A: Math. Gen. 19 3771

(http://iopscience.iop.org/0305-4470/19/18/023)

J. Phys. A: Math. Gen. 19 (1986) 3771-3784. Printed in Great Britain

Intermittency and coherent structures in two-dimensional turbulence

R Benzi†, G Paladin‡, S Patarnello†, P Santangelo† and A Vulpiani‡

† IBM ECSEC, European Center for Scientific and Engineering Computing, Via Giorgione 159, 00147 Rome, Italy

‡ Department of Physics, University of Rome 'La Sapienza', Rome, Italy and CNR, GNSM, Rome, Italy

Received 2 December 1985

Abstract. We study the mechanisms of enstrophy transfer in 2D turbulence. By theoretical discussion of the framentation process at very small scales, we show that enstrophy transfer must be space filling, due to the regularity of the flow at any time. Detailed analysis of a numerical decaying experiment confirms this picture. Yet 'intermittency' is acting at large scale due to the presence of coherent structures, namely vortices, which inhibit local enstrophy transfer.

1. Introduction

The word 'turbulence' usually refers to the chaotic motion of fluid systems at high Reynolds number. Among the various physical systems which exhibit turbulent behaviour, flows in two spatial dimensions have recently received growing attention both theoretically and experimentally. With the present generation of supercomputers it is possible to reach enough resolution to study the statistical properties of two-dimensional small scale turbulence by a direct simulation of the Navier-Stokes equations. This is still not available for three-dimensional turbulence except for a few cases with a particular spatial symmetry.

The physics of two-dimensional flows is somehow different from the three-dimensional case. For the inviscid two-dimensional case a global regularity theorem has been proved together with the uniqueness and existence theorem. Thus no singularity of the velocity field can develop in a finite time (see, for example, Rose and Sulem 1978). Moreover, besides energy, any function of vorticity, like enstrophy, is conserved. It follows that energy cannot be transferred from large to small scales in two-dimensional turbulence. Yet, in analogy with the three-dimensional case, we expect that for two-dimensional turbulence there exists an inertial range where enstrophy is cascading from large to small scales (Kraichnan 1967, Batchelor 1969). Former theories pointed out the existence of two inertial ranges: a k^{-3} enstrophy cascading range for the small scales and a $k^{-5/3}$ reverse energy cascading range for the large scales. On the other hand, numerical simulations (Basdevant *et al* 1981, McWilliams 1984) with both forcing and decaying systems show an enstrophy cascading range with a spectral slope (-4)-(-6) much steeper than -3. Basdevant *et al* (1981) argued that this difference between theoretical prediction and numerical result is due to both spatial and temporal intermittency: enstrophy dissipation is a highly fluctuating quantity whose statistical properties significantly affect the energy spectrum at small scales. Moreover,

0305-4470/86/183771+14$02.50

as noted by Basdevant *et al* (1981), Fornberg (1977) and McWilliams (1984), two-dimensional turbulence is characterised by the existence of coherent structures, namely vortices, with a lifetime much longer than their characteristic eddy turnover time. It is not clear yet which is the link between the existence of coherent structures and a strong intermittency in two-dimensional turbulence. Babiano *et al* (1984a) have tried to clarify this point by comparing the energy turbulent spectrum with the variance spectrum of a passive scalar. In the phenomenological theory a k^{-3} inertial range for the energy corresponds to a k^{-1} inertial range for the variance spectrum of the passive scalars. It turns out that while the energy spectrum has a steeper slope in the inertial range, the passive scalar develops a k^{-1} inertial range. A comparison between the vorticity field and the passive scalar field is shown in figure 3 of their paper. There is a good correlation between the two fields except at the location of the coherent vortices. One may tentatively conclude that, whatever the intermittency in two-dimensional turbulence is, coherent structures dominate the energy spectrum.

In this paper we discuss the role of intermittency in two-dimensional turbulence and its link to the formation of coherent structures. In § 2 we review the phenomenological theory in three-dimensional turbulence and compare the fractal nature of intermittency in two and three dimensions. We show that, due to the regularity of the flow at any time, at very small scales enstrophy transfer should be necessarily space filling. As already pointed out by Babiano *et al* (1984b) this result does not imply that the energy spectrum should behave with a k^{-3} slope. We speculate that enstrophy cascade can take place, at very small scales, outside coherent structures. To this end, in § 3 we analyse a numerical experiment for decaying turbulence and compute the spatial support of enstrophy cascade at different scales. We indeed find that enstrophy cascade is inhibited in the coherent structures which anyway dominate the energy spectrum for all scales. We point out the possibility of decomposing the turbulence in two parts: a background turbulence flow with a k^{-3} inertial range and no phase correlation, which almost satisfies the phenomenological theories and a finite number of vortices which advect the background field. Summary and conclusions follow in § 4.

2. Intermittency in two- and three-dimensional turbulence

As already pointed out in the introduction, three-dimensional turbulence has physical differences with respect to the two-dimensional case. We shall briefly discuss these differences with particular emphasis on the intermittency corrections to the Kolmogorov law (Kolmogorov 1941). Let $\delta v(r)$ be the velocity difference between two points at distance r. We can define the structure functions $S_p(r)$ as

$$S_p(r) \equiv \langle |\delta v(r)|^p \rangle \tag{2.1}$$

where $\langle\ \rangle$ stands for the average on the flow configuration. Then in the inertial range $S_p(r)$ obeys the scaling laws

$$S_p(r) \sim r^{\zeta_p}. \tag{2.2}$$

The values of ζ_p are related to the singularities of the velocity field. In the original Kolmogorov theory for three-dimensional turbulence $\zeta_p = p/3$ and using (2.2) we obtain

$$\lim_{r\to 0} \frac{S_1(r)}{r^{\zeta_1}} = \lim_{r\to 0} \left\langle \frac{|\delta v(r)|}{r^{1/3}} \right\rangle \neq 0 \tag{2.3}$$

which implies that $|\delta\nu(r)|/r$ is singular at very small scales. The limit $r\to 0$ means r of the order of the Kolmogorov length which goes to zero for infinite Reynolds number.

The Kolmogorov theory assumes that the set of singularities is space filling, which implies that energy dissipation is uniformly distributed in a set $A\subseteq R^3$. If we remove this assumption, as first pointed out by Landau (Landau and Lifshitz 1971), then we can take into account a correction to the Kolmogorov law induced by fluctuations of energy dissipation, namely the intermittency. This idea was first carried out by Mandelbrot (1974, 1976) and is the basis of the β model of Frisch *et al* (1978). In the β model it is assumed that

$$\lim_{r\to 0}\frac{|\delta\nu(r)|}{r^h}\neq 0 \tag{2.4}$$

where $h=(D_F-2)/3$, D_F being the fractal dimension of the set for which (2.4) holds, i.e. where energy dissipation is acting. Using (2.4) we can obtain

$$\zeta_p=\frac{D_F-2}{3}p+3-D_F. \tag{2.5}$$

In the β model, as in the Kolmogorov theory, there is only one kind of singularity and the region where energy is dissipated is a homogeneous fractal object, i.e. it has a global dilatation invariance. Frisch and Parisi (1985) pointed out that (2.5) is not consistent with experimental data (see, for example, Anselmet *et al* 1984) for $p\geqslant 7$. This is an indication that the region containing energy dissipation is not a homogeneous fractal and (2.4) holds for different h. A multifractal model has been recently proposed by Benzi *et al* (1984) and Frisch and Parisi (1985). We can simply generalise the β model in order to obtain a multifractal model and inhomogeneous fractal objects

Let us consider the scale $l_n=2^{-n}l_0$, where l_0 is the scale in which energy is injected. If at scale l_n there are N_n active eddies, each eddy $l_n(k)$ generates eddies of size $l_{n+1}(k)$ (k labels the 'father' eddy, $k=1,\ldots,N_n$). Because the rate of energy transfer is constant among $l_n(k)$ and $l_{n+1}(k)$,

$$\frac{\nu_n^3(k)}{l_n}=\beta_{n+1}\frac{\nu_{n+1}^3(k)}{l_{n+1}}. \tag{2.6}$$

Here, as in the standard β model, $\nu_n(k)$ is the velocity difference in the active eddy between two points at distance l_n and $\beta_{n+1}(k)$ is the percentage of volume occupied by the active eddies $l_{n+1}(k)$ generated by the eddy $l_n(k)$. Equation (2.6) implies that in an eddy generated by a particular set of fragmentation $\beta_1,\beta_2,\ldots,\beta_n$, the velocity difference ν_n is

$$\nu_n\sim l_n^{1/3}\left(\prod_{i=1}^{n}\beta_i\right)^{-1/3}. \tag{2.7}$$

Using (2.7) the structure functions are

$$\langle|\delta\nu(l_n)|^p\rangle=\int\prod_{i=1}^{n}\mathrm{d}\beta_i\,P(\beta_1,\beta_2,\ldots,\beta_n)\beta_i|\nu_n|^p. \tag{2.8}$$

Assuming no correlation among different steps of fragmentation (i.e. $P(\beta_1,\ldots,\beta_n)=\Pi_{i=1}^{n}P(\beta_i)$) by (2.7) and (2.8) we obtain

$$\zeta_p=\tfrac{1}{3}p-\ln_2\{\beta^{(1-p/3)}\} \tag{2.9}$$

where $\{\ \}$ indicates the average over the distribution $P(\beta)$. Note that if β is constant ($\beta = 2^{D_F - 3}$) (2.9) is equivalent to (2.5).

Naively one could think that in two-dimensional turbulence all the previous arguments can be repeated simply considering an enstrophy cascade instead of an energy cascade. This is not possible because in two-dimensional Navier-Stokes equations there are no singularities in the velocity field. Indeed it is well known for the two-dimensional Euler equation that the following inequality holds for any time (see, for example, Rose and Sulem 1978):

$$\delta v(r) \leqslant \text{constant} \times r|\ln r|. \tag{2.10}$$

This is a consequence of vorticity conservation for each fluid particle. Inequality (2.10) holds also in the Navier-Stokes equations and implies

$$\zeta_p \geqslant p. \tag{2.11}$$

Moreover, for a general theorem of probability theory (Feller 1971), ζ_p must be a convex function of p. Assuming $\zeta_3 = 3$ (i.e. a constant forward enstrophy cascade) (2.11) and convexity of ζ_p one obtains (apart from logarithmic corrections) the result

$$\zeta_p = p. \tag{2.12}$$

Thus we obtain the apparently surprising result that in two-dimensional turbulence the Kolmogorov scaling law (2.12) holds also in the presence of intermittency. Note that, except for the Kolmogorov law ($\beta_n = 1$), any random β model gives wrong results in two-dimensional turbulence. Indeed we can repeat the considerations done for the three-dimensional case using the assumption of constant enstrophy transfer rate. In this case equation (2.6) becomes

$$\frac{v_n^3(k)}{l_n^3} = \beta_{n+1} \frac{v_{n+1}^3(k)}{l_{n+1}^3}. \tag{2.13}$$

By (2.13) we obtain for ζ_p a convex function $\zeta_3 = 3$ and consequently inequality (2.11) is broken by the singularities bearing in the fragmentation mechanism. We remark that this undesired result (i.e. the appearance of singularities of the velocity field) is due to the fact that in the fragmentation process β_n is not independent of β_{n-1}, to the Bernoullian nature of the random β model. Let us consider a simple modification to the cascade model in order to satisfy (2.12). We still consider a constant enstrophy transfer rate, i.e. (2.13), but with the further constraint

$$\beta_{n+1}(k) = 1 \qquad \text{if } v_n^3/l_n^3 \geqslant \eta_{\max} \tag{2.14}$$

where $\eta_{\max}$ is a bound to the enstrophy transfer which reflects the constraint (2.10).

With (2.14) the fragmentation process now has a Markovian nature because the steps of the cascade depend on the previous ones. We think that constraint (2.14) is the simplest way, at least in fragmentation models, to avoid singularities. It is easy to see that with this model we obtain $\zeta_p = p$. Indeed the regions where enstrophy dissipation is concentrated have fractal dimension equal to 2, i.e. they occupy an area non-decreasing for decreasing scale length. Roughly speaking we do not have a multifractal anymore but a 'checkers'-like structure, at least at very small scales. We remark that, unlike three-dimensional turbulence, in the two-dimensional case it is not possible to get information on the behaviour of the energy spectrum $E(k)$ from a

knowledge of ζ_p. With naive dimensional arguments one could conclude that $E(k) \sim k^{-1-\zeta_2}$ but this conclusion is wrong if $\zeta_2 \geqslant 2$ (see, for example, Babiano *et al* 1984b). Therefore the only result from the bound (2.10) is that

$$E(k) \sim k^{-\alpha} \qquad \alpha \geqslant 3. \tag{2.15}$$

Moreover, neither the value of α nor the structure functions (in fact $\zeta_p = p$) can give information about intermittency in two-dimensional turbulence.

3. Numerical experiments

For two-dimensional turbulent flows at very high Reynolds number, energy is conserved and enstrophy is dissipated. This asymptotic limit is never achieved in the numerical experiments because of truncation effects. Recently Sadourny and Basdevant (1981) have introduced the technique of anticipated vorticity for the numerical simulation of enstrophy dissipation (see also Leith 1985). Let ω be the vorticity and ψ its stream function. ω satisfies the equation

$$\partial_t \omega + J(\psi, \omega) = D + F \tag{3.1}$$

where

$$\omega = \Delta\psi \tag{3.2}$$

where D is dissipation and F is forcing. A simple way to dissipate enstrophy but not energy is to assume that D is proportional to $J(\psi, \omega^*)$ where ω^* represents physically the vorticity of not resolved scales at which viscosity is acting. It follows that for $F = 0$

$$\partial_t \int \tfrac{1}{2}\omega^2 \, dx \, dy = \int \omega J(\psi, \omega^*) \, dx \, dy = -\int \omega^* J(\psi, \omega) \, dx \, dy. \tag{3.3}$$

Basdevant and Sadourny (1983) assumed that

$$-\omega^* = \theta L[J(\psi, \omega)] \tag{3.4}$$

where L is a positive linear operator and θ is a parameter. With (3.4) equation (3.1) becomes

$$\partial_t \omega + J(\psi, \omega) - \theta J(\psi, L(J(\psi, \omega))) = F. \tag{3.5}$$

We have performed a numerical simulation of equation (3.5) with $F = 0$, i.e. for decaying turbulence. We have chosen for the operator L the form Δ^{2p}, with $p = 1$ and $\theta = 6 \times 10^{-10}$. The numerical model is a periodic spectral model (128×128 grid points) with the Patterson and Orszag (1971) dealiasing procedure applied to the computation of the Jacobian. The initial conditions are the same as in McWilliams' (1984) experiment, i.e. a random initial configuration with an asymptotic energy spectrum $\sim k^{-3}$, a total energy $E = 0.5$ and a size of the grid 2π. Figure 1 shows the behaviour of enstrophy, which is slowly decreasing in time, while energy is conserved to five digit accuracy in our computation. Figures 2-5 show the vorticity at four different times. As the system is decaying we see the emergence of 'isolated coherent vortices' in the flow (McWilliams 1984). Meanwhile the energy spectrum shows an inertial range with a slope steeper

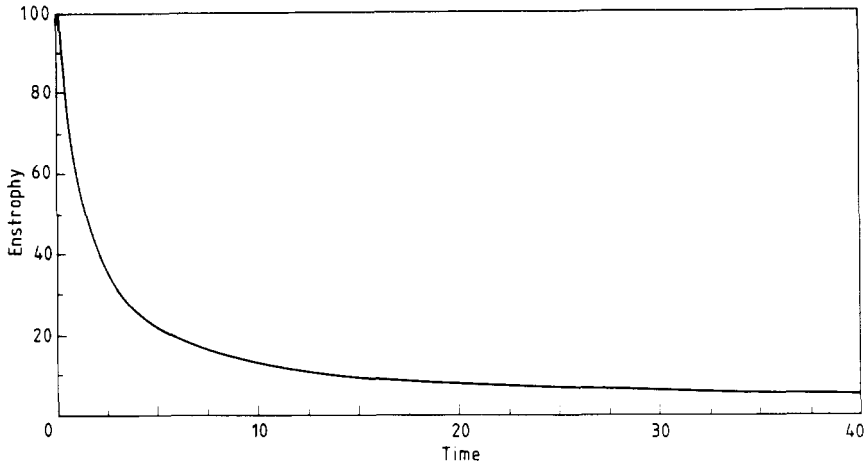

Figure 1. Enstrophy as a function of time for the 128×128 spectral run with anticipated vorticity scheme (AVS).

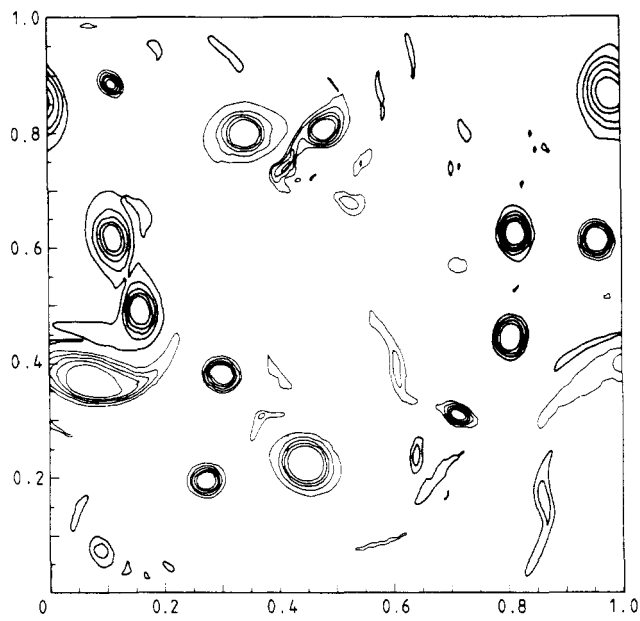

Figure 2. Vorticity contours at $t = 20$ time units for the AVS run. The following contours are shown: -10, -8, -6, -4, -2 (fine lines) and 2, 4, 6, 8, 10 (bold lines).

than -3 as shown in figure 6. It is useful to compare figures 4 and 6 with an experiment for which a superviscosity $\nu\Delta\Delta\omega$ is used instead of the anticipated vorticity scheme. Figures 7 and 8 refer to the numerical simulation of equation

$$\partial_t\omega + J(\psi, \omega) = -\nu\Delta\Delta\omega \tag{3.6}$$

with the same initial condition of equation (3.5). We see that the energy spectrum in figure 8 shows almost the same slope as the simulation with anticipated vorticity (figure

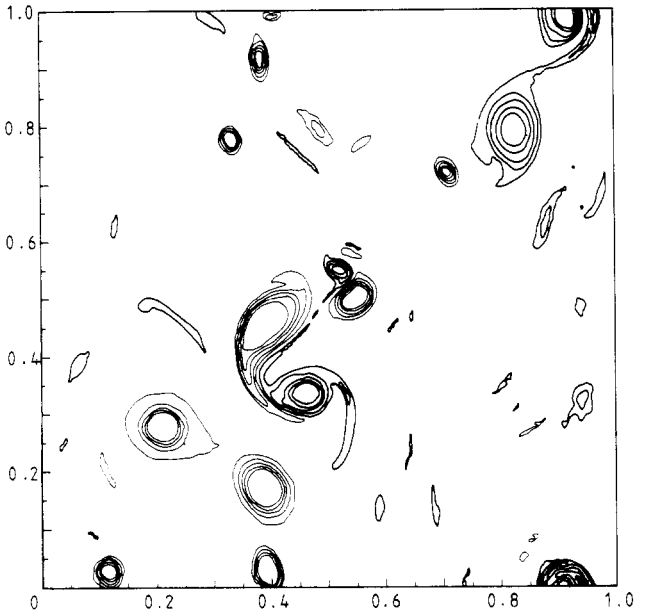

Figure 3. The same as in figure 2 at $t = 25$.

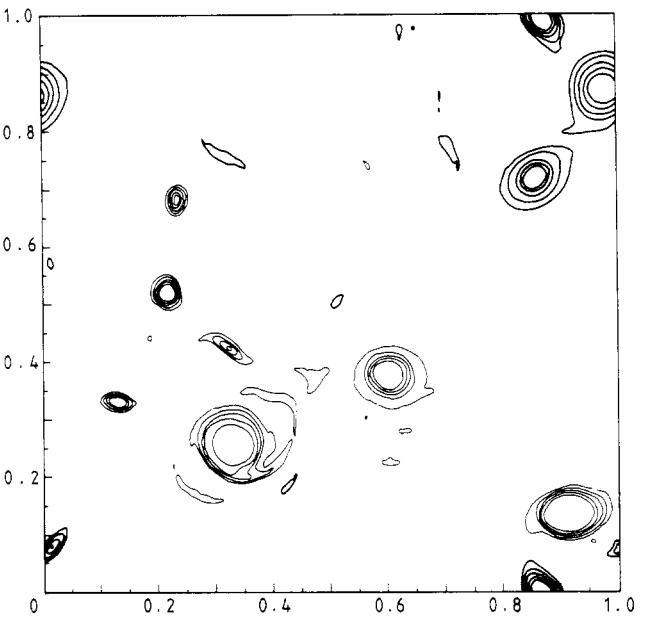

Figure 4. The same as in figure 2 at $t = 30$.

6) but with a marked dissipative range for large k. At the same time the vorticity field (figure 7) shows coherent vortices with a somehow larger scale with respect to that of figure 4. The inertial range simulated with the anticipated vorticity is characterised by the constant flux of enstrophy form large to small scales even for very large values of k. To study its spatial support we proceed as follows. For any interval $[k - \delta k, k + \delta k]$

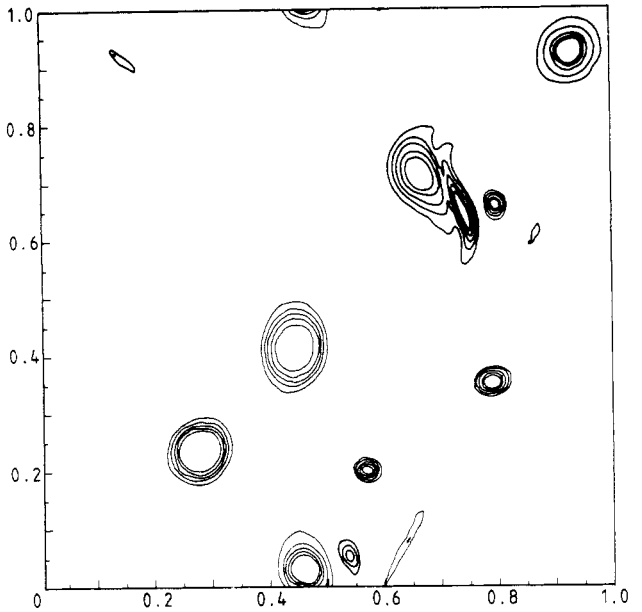

Figure 5. The same as in figure 2 at $t = 35$.

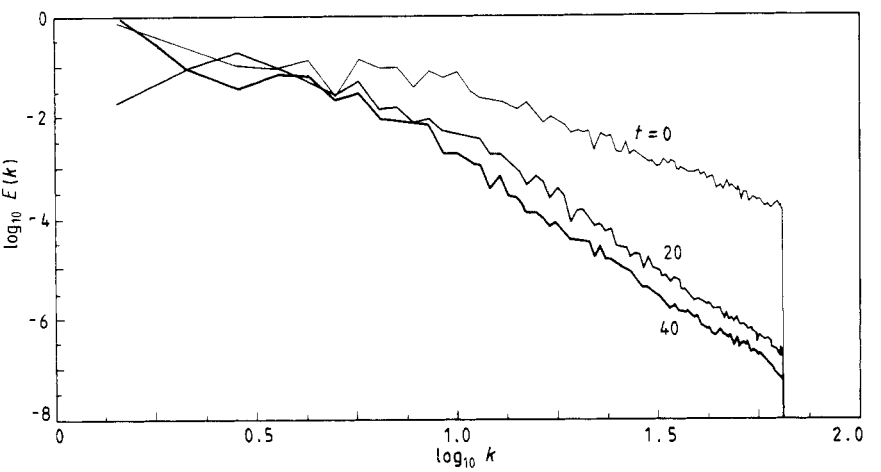

Figure 6. Energy spectra for the AVS run at $t = 0$, 20, 40.

in the Fourier space we decompose the stream function into three parts:

$$\psi = \psi_{k'} + \psi_k + \psi_{k''} \tag{3.7}$$

where

$$\psi_{k'} = \int_{0 \leqslant |\boldsymbol{p}| \leqslant k - \delta k} \hat{\psi}(\boldsymbol{p}) \exp(-\mathrm{i}\boldsymbol{p} \cdot \boldsymbol{x}) \, \mathrm{d}\boldsymbol{p}$$

$$\psi_k = \int_{k - \delta k \leqslant |\boldsymbol{p}| \leqslant k + \delta k} \hat{\psi}(\boldsymbol{p}) \exp(-\mathrm{i}\boldsymbol{p} \cdot \boldsymbol{x}) \, \mathrm{d}\boldsymbol{p}$$

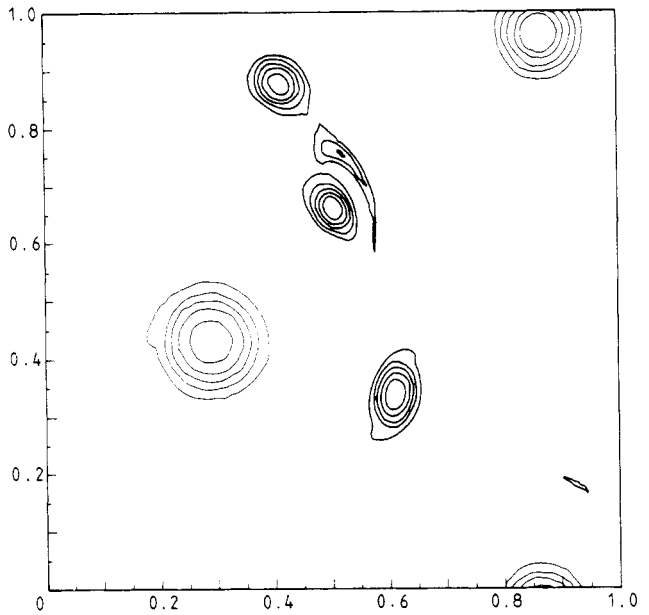

Figure 7. Vorticity contours for the spectral 128×128 run with superviscosity dissipation scheme with $\nu = 5 \times 10^{-7}$ at $t = 30$. The contours are the same as in figure 2. The comparison with figure 4 shows less detail on small scales.

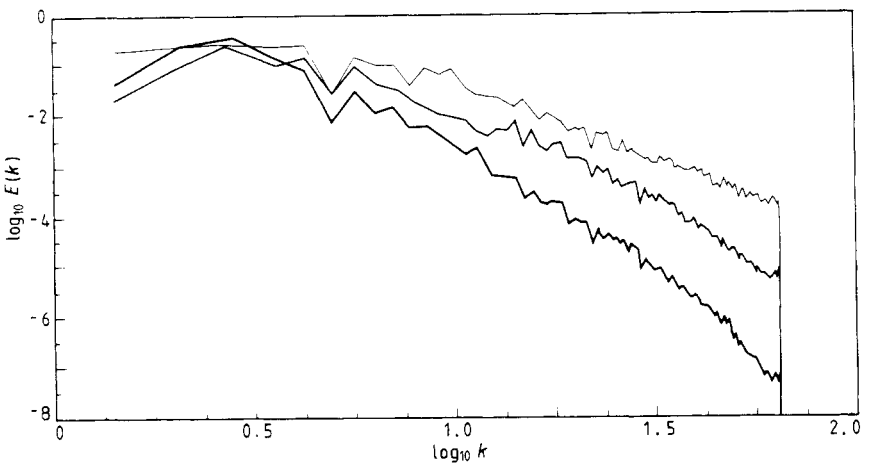

Figure 8. Energy spectra for the superviscosity run at $t = 0, 20, 40$.

$$\psi_{k''} = \int_{k+\delta k \leq |\boldsymbol{p}| \leq k_M} \hat{\psi}(\boldsymbol{p}) \exp(-\mathrm{i}\boldsymbol{p} \cdot \boldsymbol{x}) \, \mathrm{d}\boldsymbol{p}$$

$\hat{\psi}(\boldsymbol{p})$ is the Fourier transform of $\psi(\boldsymbol{x})$ and k_M is the maximum value of k available in the numerical experiment (in our case 64). We can also decompose ω in a similar way:

$$\omega = \omega_{k'} + \omega_k + \omega_{k''}. \tag{3.8}$$

Equation (3.5) then becomes

$$\partial_t \omega_{k'} + \partial_t \omega_k + \partial_t \omega_{k''} + J(\psi, \omega_{k'} + \omega_{k''}) + J(\psi, \omega_k) = D. \tag{3.9}$$

Let us now define P_k the projector operator on the Fourier modes in the interval $[k - \delta k, k + \delta k]$. It follows that

$$\partial_t \omega_k + P_k[J(\psi, \omega_{k'} + \omega_{k''}) + J(\psi, \omega_k) - D] = 0. \tag{3.10}$$

The enstrophy in the range $[k - \delta k, k + \delta k]$ is given by $\Omega(k) = \int \omega_k^2 \, dx \, dy$. Hence

$$\tfrac{1}{2}\partial_t \Omega(k) = -\int \omega_k P_k[J(\psi, \omega_{k'} + \omega_{k''})] \, dx \, dy$$

$$- \int \omega_k P_k[J(\psi, \omega_k)] \, dx \, dy + \int \omega_k P_k[D] \, dx \, dy. \tag{3.11}$$

The second integral on the RHS of equation (3.11) vanishes identically. The first and the third have a clear physical meaning. The third integral parametrises dissipation effects. Thus enstrophy cascade is due to the first integral on the RHS of equation (3.11) and the field $\omega_k P_k[J(\psi, \omega_{k'} + \omega_{k''})]$ is the support of enstrophy cascade.

In the following computation we choose $\delta k = 5$. Figure 9 shows the field $\eta_k = \omega_k P_k[J(\psi, \omega_{k'} + \omega_{k''})]$ for different values of k computed at time $t = 35$. The vorticity field is shown in figure 5. A strong enstrophy cascade is acting in the region where the two vortices on the upper right-hand corner of figure 5 are merging. This cascade is displayed for all the computed values of k showing that there is no time lag between the field η_k and the position of the vortices. The merging of the vortices is a characteristic of the transient behaviour of the simulation that, we recall, refers to a decaying experiment. Going from figure 9(a) to 9(h) we see that enstrophy transfer is initially located in correspondence of the coherent structures but eventually quite a large area is filled uncorrelated or even negatively correlated with the position of vortices. We can compute the area of the 'active' region A^* of enstrophy transfer using as a definition of A^*, for each k band, the area for which η_k is greater than 10% of its maximum. We remark that this definition of A^* is quite arbitrary but it seems reasonable for our purpose. The behaviour of $A^*(k)$ is shown in figure 10. The most interesting feature of this figure is the minimum of $A^*(k)$ for $k \sim 20$-30. This value of k corresponds to the decorrelation between the field η_k and the coherent structures as we can see from figure 9. We can argue that enstrophy cascade is somehow stopped in the region of coherent vortices and for larger values of k the enstrophy transfer is acting outside these regions. We note that the growing of $A^*(k)$ for $k \geq 20$-30 could be due to our empirical definition of A^*. To clarify the scenario we plot in figure 11 the values of $\sup_{xy} |\eta_k(x, y)|$ which is sharply decreasing for $k < 20$-30 and almost constant $k \geq 20$-30. This behaviour of $\sup_{xy} |\eta_k|$ is consistent with an increase of $A^*(k)$ because a constant flux of enstrophy transfer is indeed observed in the inertial range. It follows by the above considerations (regardless the definition of $A^*(k)$) that at $k \geq 20$-30 the enstrophy cascade shows a quite sharp transition in its spatial behaviour. This result seems qualitatively in agreement with the considerations discussed in § 2 even if we cannot conclude that the spatial support of enstrophy cascade is space filling. One may wonder why the energy spectrum does not show any quantitative difference in the range $k \sim 20$-30 (see figure 6). Following Basdevant *et al* (1985) we decompose the vorticity field into two parts: the coherent structures and the background field. We define the coherent structures as

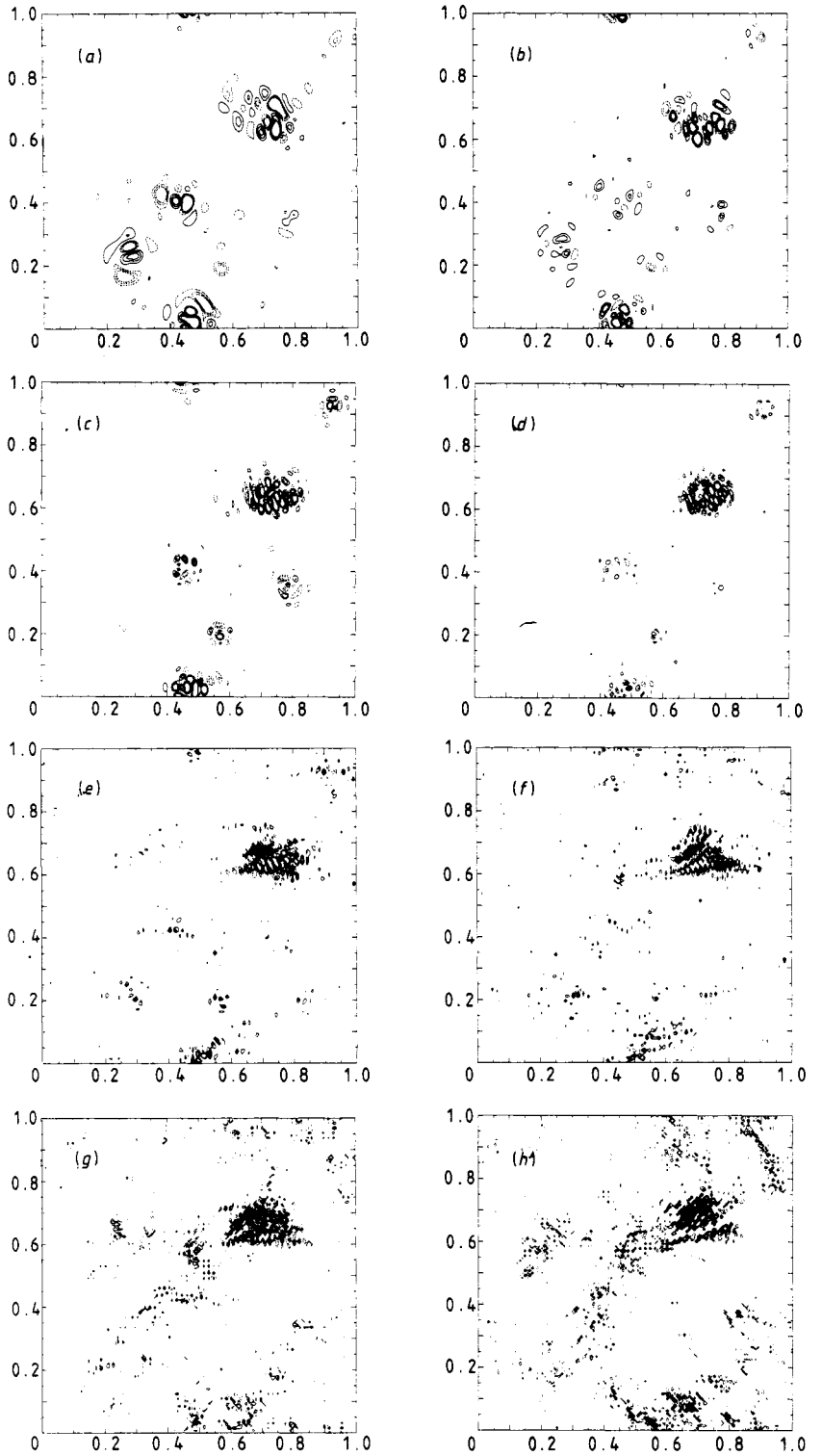

Figure 9. Contour maps of the field $\eta_k = \omega_k P_k[J(\psi, \omega_{k'} + \omega_{k''})]$, which is the support of enstrophy transfer for the scale k (see § 3). The maps refer to the AVS run at $t = 35$. The following wavenumber bands are shown: (*a*) 5-15, (*b*) 10-20, (*c*) 15-25, (*d*) 20-30, (*e*) 25-35, (*f*) 30-40, (*g*) 35-45, (*h*) 40-50. For each map the contours corresponding to 10%, 20% and 30% of the maximum (full lines) and 10%, 20% and 30% of the minimum (broken lines) are shown.

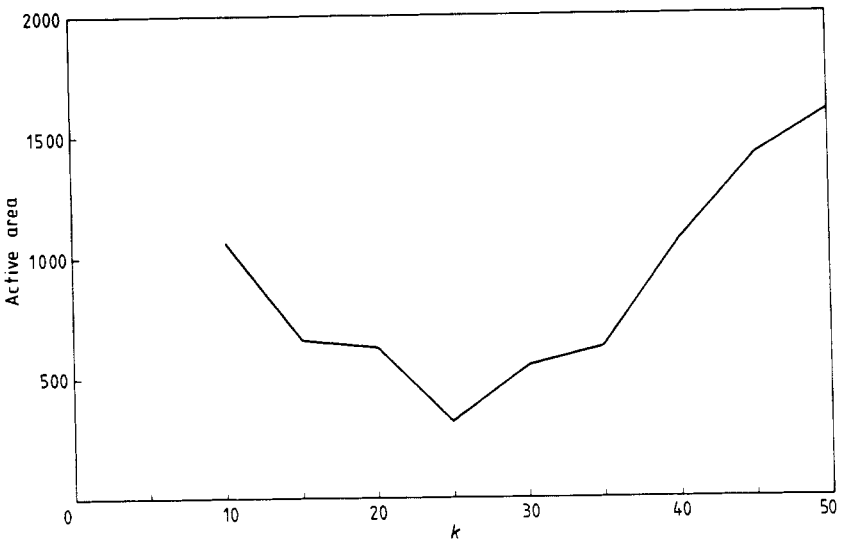

Figure 10. 'Active' area against wavenumber k for the configuration of figure 4.

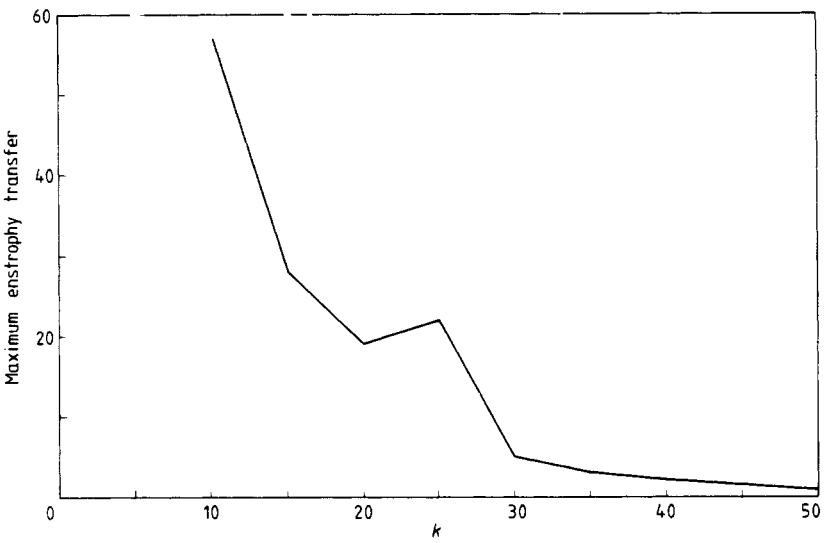

Figure 11. Maximum value of the enstrophy transfer field for the configuration of figure 4.

$$\omega_c = \begin{cases} \omega(x,y) & \text{for } |\omega(x,y)| > \omega_{th} \\ \omega_{th} & \text{for } |\omega(x,y)| \leq \omega_{th} \text{ and } \omega(x,y) > 0 \\ -\omega_{th} & \text{for } |\omega(x,y)| \leq \omega_{th} \text{ and } \omega(x,y) < 0 \end{cases} \tag{3.12}$$

and the background field as

$$\omega_b = \begin{cases} \omega(x,y) & \text{for } |\omega(x,y)| < \omega_{th} \\ \omega_{th} & \text{for } |\omega(x,y)| \geqslant \omega_{th} \text{ and } \omega(x,y) > 0 \\ -\omega_{th} & \text{for } |\omega(x,y)| \geqslant \omega_{th} \text{ and } \omega(x,y) < 0 \end{cases} \tag{3.13}$$

where ω_{th} is a threshold value ~20% of the maximum absolute value of the vorticity.

Figures 12 and 13 show the energy spectrum related to ω_c and ω_b. We note that the background field has a k^{-3} inertial range and the coherent structures show a k^{-5} behaviour for $k \leqslant 20$–30 and a k^{-3} at very small scales. Moreover, for large k the energy spectrum for the coherent structures and the background field are of the same order of magnitude. Although our decomposition can be questionable, the results shown in figures 12 and 13 are consistent with what it is observed in figure 9. The background turbulent field is dynamically active at large k and the power spectrum is dominated by the coherent vortices. Invoking the numerical result of Babiano *et al* (1984a) on the dynamics of a passive scalar, it is tempting to conclude that the background is mainly advected by the coherent structures and that the motion of the vortices is mainly due to vortex–vortex interactions and to small, probably random, perturbations induced by the background field. The background field should have a k^{-3} inertial range and a space filling fragmentation for enstrophy transfer. If we think of intermittency as a fluctuation in the enstrophy cascade then vortices are large scale intermittent configurations because they seem to inhibit the cascade process.

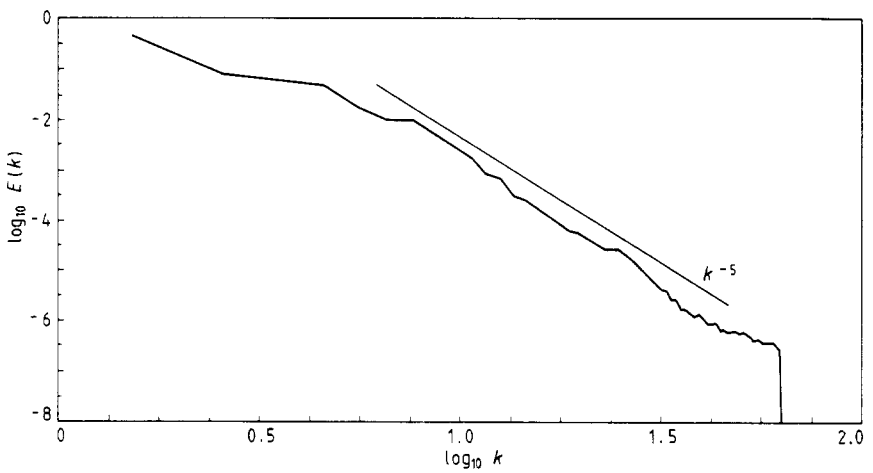

Figure 12. Energy spectra for ω_c (see equation (3.12)) for the configuration of figure 4.

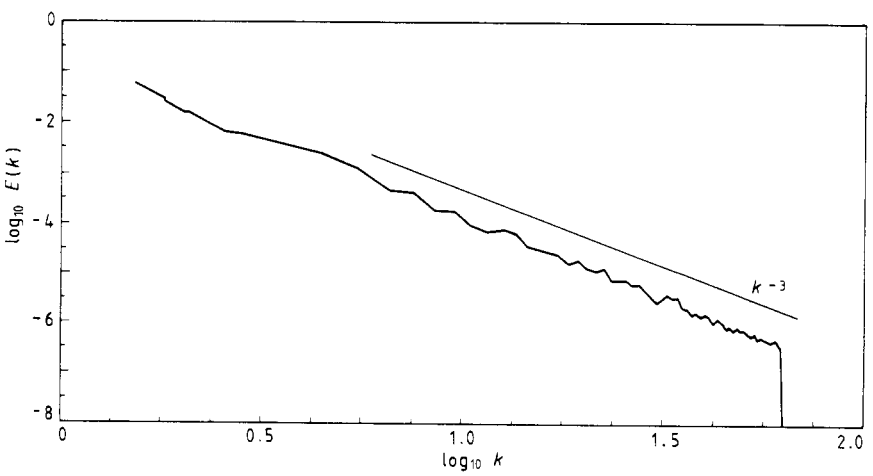

Figure 13. Energy spectra for ω_b (see equation (3.13)) for the configuration of figure 4.

4. Summary and conclusions

In this paper we have analysed the enstrophy cascade process in two-dimensional turbulent flow. We give quite general arguments to state that a small scale cascade should be space filling, i.e. no intermittency is active at very small scale. On the other hand, coherent structures seem to stop locally the cascade process. We find a scale separation between enstrophy cascade locally induced by the coherent vortices and that acting in the background field. The only exception to this case is due to vortex merging, which produces enstrophy cascade throughout the inertial range. Vortices seem to be 'cold' structures at very small scale and this can partially explain their stability for times longer than their characteristic eddy turnover time. The background field seems to obey a Kolmogorov theory with a k^{-3} law. The whole picture which is emerging is that there is a possible dynamical decomposition of two-dimensional turbulent flow: few degrees of fredom (namely the vortices) interacting mainly with each other and a background field advected by the vortices and dynamically active only at very small scales. The statistical properties of the background field could be inferred by closure theories which, in absence of intermittency, are good candidates to model the system. Higher resolution experiments are in progress to verify the consistency of the above scenario.

References

Anselmet F, Gagne Y, Hopfinger E J and Antonia R A 1984 *J. Fluid Mech.* **140** 63
Babiano A, Basdevant C, Legras B and Sadourny R 1984 *C.R. Acad. Sci., Paris* B **299** 601
Babiano A, Basdevant C and Sadourny R 1984b *C.R. Acad. Sci., Paris* B **299** 495
Basdevant C, Legras B and Sadourny R 1985 Private communication
Basdevant C, Legras B, Sadourny R and Beland M 1981 *J. Atmos. Sci.* **38** 2305
Basdevant C and Sadourny R 1983 *J. Mech. Teor. Appl.* **243** (special issue)
Batchelor G K 1969 *Phys. Fluids Suppl. 2* **12** 233
Benzi R, Paladin G, Parisi G and Vulpiani A 1984 *J. Phys. A: Math. Gen.* **17** 3521
Feller W 1971 *An Introduction to Probability Theory and its Applications* vol 2 (New York Wiley)
Fornberg B 1977 *J. Comp. Phys.* **25** 1
Frisch U and Parisi G 1985 *Turbulence and Predictability in Geophysical and Fluid Dynamics* ed M Ghil, R Benzi and G Parisi (Amsterdam: North-Holland) p 71
Frisch U, Sulem P L and Nelkin M 1978 *J. Fluid Mech.* **87** 719
Kolmogorov A N 1941 *C.R. Acad. Sci., URSS* **30** 301
Kraichnan R H 1967 *Phys. Fluids* **10** 1417
Landau L D and Lifschitz L 1971 *Mecanique des Fluides* (Moscow: MIR)
Leith C E 1985 *Turbulence and Predictability in Geophysical and Fluid Dynamics* ed M Ghil, R Benzi and G Parisi (Amsterdam: North-Holland) p 266
McWilliams J C 1984 *J. Fluid Mech.* **146** 21
Mandelbrot B 1974 *J. Fluid Mech.* **62** 331
—— 1976 *C.R. Acad. Sci., Paris* **282a** 119
Patterson G S Jr and Orszag S 1971 *Phys. Fluids* **14** 2538
Rose H A and Sulem P L 1978 *J. Physique* **39** 441
Sadourny R and Basdevant C 1981 *C.R. Acad. Sci., Paris* **292** 1061